J|A|C|S
ARTICLES
Published on Web 08/10/2006

Triconstituent Co-assembly to Ordered Mesostructured Polymer−Silica and Carbon−Silica Nanocomposites and Large-Pore Mesoporous Carbons with High Surface Areas

Ruili Liu,[†] Yifeng Shi,[†] Ying Wan,[†,‡] Yan Meng,[†] Fuqiang Zhang,[†] Dong Gu,[†] Zhenxia Chen,[†] Bo Tu,[†] and Dongyuan Zhao*[,†,§,#]

Contribution from the Department of Chemistry, Shanghai Key Laboratory of Molecular Catalysis and Innovative Materials, Key Laboratory of Molecular Engineering of Polymers, and Advanced Materials Laboratory, Fudan University, Shanghai 200433, People's Republic of China, and Department of Chemistry, Shanghai Normal University, Shanghai 200234, People's Republic of China

Received May 14, 2006; E-mail: dyzhao@fudan.edu.cn

Abstract: Highly ordered mesoporous polymer−silica and carbon−silica nanocomposites with interpenetrating networks have been successfully synthesized by the evaporation-induced triconstituent co-assembly method, wherein soluble resol polymer is used as an organic precursor, prehydrolyzed TEOS is used as an inorganic precursor, and triblock copolymer F127 is used as a template. It is proposed for the first time that ordered mesoporous nanocomposites have "reinforced concrete"-structured frameworks. By adjusting the initial mass ratios of TEOS to resol, we determined the obtained nanocomposites possess continuous composition with the ratios ranging from zero to infinity for the two constituents that are "homogeneously" dispersed inside the pore walls. The presence of silicates in nanocomposites dramatically inhibits framework shrinkage during the calcination, resulting in highly ordered large-pore mesoporous carbon−silica nanocomposites. Combustion in air or etching in HF solution can remove carbon or silica from the carbon−silica nanocomposites and yield ordered mesoporous pure silica or carbon frameworks. The process generates plenty of small pores in carbon or/and silica pore walls. Ordered mesoporous carbons can then be obtained with large pore sizes of ∼6.7 nm, pore volumes of ∼2.0 cm^3/g, and high surface areas of ∼2470 m^2/g. The pore structures and textures can be controlled by varying the sizes and polymerization degrees of two constituent precursors. Accordingly, by simply tuning the aging time of TEOS, ordered mesoporous carbons with evident bimodal pores at 2.6 and 5.8 nm can be synthesized.

1. Introduction

A broad range of scientific endeavors has established a growing interest in nanoscience, mainly due to the new and unpredictable properties of nanomaterials and the ability to controllably design and fabricate materials on nanoscale. In these regards, nanocomposites have drawn more and more attention. Two or more phases can be combined together that historically have been viewed as very different and even incompatible, and each of the domain sizes is below 100 nm. The resulting materials are more homogeneous than conventional hybrid materials and generate remarkable and complementary properties, which cannot be obtained in a single component.[1−5] For example, organic−inorganic nanocomposites carry the advantages both of organic polymers like flexibility, toughness, hydrophobicity, and versatility for further functionalization, and of inorganic components such as good mechanical and thermal stability. Similarly, mesoporous carbon−silica nanocomposites can also improve thermal, chemical, conductive, and mechanical properties. Confined-space effects inside the nanospace of mesostructures would certainly modify the unique chemical behaviors of polymer−silica[4−7] and carbon−silica[8−10] nanocomposites, which have inspired chemists and material scientists to create mesoporous nanocomposites. It would provide an opportunity to develop porous materials for specific applications, such as in catalysis, adsorption, optics devices, and electrodes.[4,5,9,10]

[†] Department of Chemistry and Shanghai Key Laboratory of Molecular Catalysis and Innovative Materials, Fudan University.
[§] Key Laboratory of Molecular Engineering of Polymers, Fudan University.
[#] Advanced Materials Laboratory, Fudan University.
[‡] Shanghai Normal University.

(1) Wei, Y.; Jin, D. L.; Yang, C. C.; Kels, M. C.; Qiu, K. Y. *Mater. Sci. Eng., C* **1998**, *6*, 91.
(2) Nagarale, R. K.; Gohil, G. S.; Shahi, V. K.; Rangarajan, R. *Macromolecules* **2004**, *37*, 10023.
(3) Chen, M.; Zhou, S. X.; You, B.; Wu, L. M. *Macromolecules* **2005**, *38*, 6411.
(4) Choi, M.; Kleitz, F.; Liu, D. N.; Lee, H. Y.; Ahn, W. S.; Ryoo, R. *J. Am. Chem. Soc.* **2005**, *127*, 1924.
(5) Scott, B. J.; Wirnsberger, G.; Stucky, G. D. *Chem. Mater.* **2001**, *13*, 3140.
(6) Asefa, T.; MacLachan, M. J.; Coombs, N.; Ozin, G. A. *Nature* **1999**, *402*, 867.
(7) Inagaki, S.; Guan, S.; Fukushima, Y.; Ohsuna, T.; Terasaki, O. *J. Am. Chem. Soc.* **1999**, *121*, 9611.
(8) Anderson, M. L.; Stroud, R. M.; Rolison, D. R. *Nano Lett.* **2002**, *2*, 235.
(9) Mastai, Y.; Polarz, S.; Antonietti, M. *Adv. Funct. Mater.* **2002**, *12*, 197.
(10) Tsionsky, M.; Gun, G.; Glezer, V.; Lev, O. *Anal. Chem.* **1994**, *66*, 17473.

10.1021/ja0633518 CCC: $33.50

Ordered mesoporous organic−silica nanocomposites have been achieved by surface functionalization,[11,12] encapsulation of organic moieties in the channels of mesoporous silica materials,[4,13] and direct synthesis of periodic mesoporous organosilicas (PMOs).[6,7] Functionalized mesoporous silicates can be synthesized either by using organosilanes and/or tetraethyl orthosilicate (TEOS) as precursors[11] or by using functional surfactants.[12] One drawback is that organosilanes and functional surfactants are expensive and difficult to obtain. Other drawbacks are that organic functional groups may block the pores and their random distributions limit further applications. The pore-blocked problem also exists in the method of encapsulation of organic moieties, especially polymers. It requires careful control of the polymerization to avoid imbuing with polymers.[4,13] An extra step is sometimes necessary to prepare silica frameworks. PMOs represent a new kind of ordered mesostructures derived from surfactant-templated condensation of bridged bifunctional organosiloxane precursors.[6,7,14] Integrating organic groups including methylene, ethane, ethylene, and benzene into inorganic solid pore walls is achieved in one step, which leaves pore voids and improves the smooth accessibility of functional sites. Nevertheless, the bridged bifunctional organosiloxane precursors make the synthesis uneconomic. Inherent hydrophobic character in high organic-content precursors leads to either a phase separation or disordered materials.[14,15]

On the inheritance of synthetic procedures of organic−silica nanocomposites, direct carbonization and adding carbon particles to silica networks can yield mesoporous carbon−silica nanocomposites.[4,16] Random distributions of two constituents, pore blockage, or uneconomic processes are also derived. Co-assembly of inorganic and organic phases from the sol−gel process and subsequent carbonization is a facile method to prepare carbon−silica nanocomposites.[17,18] Most carbon−silica nanocomposites are, however, disordered. It is possibly because of the different polymerization rates of inorganic and organic species, which destroy their co-assembly and lead to disordered arrangements. Simultaneously, phase separation occurs in a large area. The products lack the merits of composites. From the viewpoint of synthesis, it is a challenge to get ordered mesoporous nanocomposites using a one-step, convenient, and economic approach. The embedded constituents can therefore actually be controlled, and the synthesis is reproducible. Finally, the results can be predicted.

Recently, highly ordered mesoporous polymers and carbons have been reported by several research groups, which were synthesized from block copolymers self-assembly.[19−23] Notably, when low-molecular-weight and water-soluble phenolic resins (resols) are used as precursors, highly ordered mesostructures with covalent-bond polymer infinite frameworks can be easily obtained from organic−organic assembly, which is comparable to that for mesoporous silica from inorganic−organic assembly. In addition, this approach to ordered mesoporous carbon molecular sieves overcomes the shortages of conventional two-step synthesis of mesoporous carbon replicas by nanocasting,[24−26] which is laborious, time-consuming, and costly. However, serious skeleton shrinkage during the high-temperature carbonization procedure results in low surface areas, small pore sizes, and low pore volumes for mesoporous carbon products. An implied advantage for the incorporation of a rigid constituent of silica in polymer−silica nanocomposites is the effective reduction of framework shrinkage,[27] which would facilitate one to prepare carbon−silica nanocomposites with large pore sizes. Further removing silica can lead to large-pore mesoporous carbons.

Herein, we demonstrate a triconstituent co-assembly approach to prepare well-ordered mesoporous polymer−silica and carbon−silica nanocomposites by using resols as a polymer precursor, silicate oligomers as an inorganic precursor, and triblock copolymer F127 as a template. This process is easy and reproducible. Hybrid nanocomposite products have "homogeneous" interpenetrating frameworks and large pores (∼8.5 nm). A controllable composition diagram in the nanocomposites can be drawn from 0 to 1, that the mass ratios of polymer−resin/silica or carbon/silica range from zero to infinity. The presence of rigid silicates in the nanocomposites can greatly reduce structural shrinkage during the calcination. After the removal of carbon by simple combustion or removal of silica by HF etching from carbon−silica nanocomposites, ordered mesoporous pure silica or carbon frameworks can be obtained. The ordered carbon products have interconnected pores with uniform pore sizes as large as 6.7 nm and surface areas as high as 2470 m^2/g. By prolonging the aging time of TEOS, highly ordered mesoporous carbon can be synthesized with obvious bimodal pores at 2.6 and 5.8 nm, respectively. A "reinforced-concrete" framework structure for the nanocomposites is proposed. Ordered mesoporous carbons with high surface areas, large pore sizes and pore volumes, and interconnected pore structures would benefit their practical applications, such as electrodes for electric double-layer capacitors and adsorbents for proteins, vitamins, or dyes.

2. Experimental Section

2.1. Chemicals. Poly(propylene oxide)-*block*-poly(ethylene oxide)-*block*-poly(propylene oxide) triblock copolymer Pluronic F127 (M_w = 12 600, $PEO_{106}PPO_{70}PEO_{106}$) was purchased from Acros Corp. Tetraethyl orthosilicate (TEOS), phenol, formalin solution (37 wt %), NaOH, HCl, and ethanol were purchased from Shanghai Chemical Corp. All chemicals were used as received without any further purification. Millipore water was used in all experiments.

(11) Shimojima, A.; Liu, Z.; Ohsuna, T.; Terasaki, O.; Kuroda, K. *J. Am. Chem. Soc.* **2005**, *127*, 14108.
(12) Yang, Y.; et al. *J. Am. Chem. Soc.* **2003**, *125*, 1269.
(13) Yoon, S. B.; Kim, J. Y.; Yu, J. S. *Chem. Commun.* **2002**, 1536.
(14) Hunks, W. J.; Ozin, G. A. *Chem. Mater.* **2004**, *16*, 5465.
(15) Sayari, A.; Wang, W. H. *J. Am. Chem. Soc.* **2005**, *127*, 12194.
(16) Pang, J. B.; John, V. T.; Loy, D. A.; Yang, Z. Z.; Lu, Y. F. *Adv. Mater.* **2005**, *17*, 704.
(17) Wang, Z. M.; Hohsinoo, K.; Shishibori, K.; Kanoh, H.; Ooi, K. *Chem. Mater.* **2003**, *15*, 2926.
(18) Lee, J.; Kim, J.; Lee, Y.; Yoon, S.; Oh, S. M.; Hyeon, T. *Chem. Mater.* **2004**, *16*, 3323.
(19) Liang, C. D.; Hong, K. L.; Guiochon, G. A.; Mays, J. W.; Dai, S. *Angew. Chem., Int. Ed.* **2004**, *43*, 5785.
(20) Tanaka, S.; Nishiyama, N.; Egashira, Y.; Ueyama, K. *Chem. Commun.* **2005**, 2125.
(21) Meng, Y.; Gu, D.; Zhang, F. Q.; Shi, Y. F.; Yang, H. F.; Li, Z.; Yu, C. Z.; Tu, B.; Zhao, D. Y. *Angew. Chem., Int. Ed.* **2005**, *44*, 7053.
(22) Zhang, F. Q.; Meng, Y.; Gu, D.; Yan, Y.; Yu, C. Z.; Tu, B.; Zhao, D. Y. *J. Am. Chem. Soc.* **2005**, *127*, 13508.
(23) Liang, C.; Dai, S. *J. Am. Chem. Soc.* **2006**, *128*, 5316.
(24) Ryoo, R.; Joo, S. H.; Jun, S. *J. Phys. Chem. B* **1999**, *103*, 7743.
(25) Jun, S.; Joo, S. H.; Ryoo, R.; Kruk, M.; Jaroniec, M.; Liu, Z.; Ohsuna, T.; Terasaki, O. *J. Am. Chem. Soc.* **2000**, *122*, 10712.
(26) Joo, S. H.; Choi, S. J.; Oh, I.; Kwak, J.; Liu, Z.; Terasaki, O.; Ryoo, R. *Nature* **2001**, *412*, 169.
(27) Wei, Y.; Jin, D. L.; Yang, C. C.; Wei, G. *J. Sol.-Gel Sci. Technol.* **1996**, *7*, 191.

Table 1. Preparation Conditions and Composites of the Ordered Mesostructured Polymer−Silica and Carbon−Silica Nanocomposites by Triconstituent Co-assembly via the EISA Method, and of the Corresponding Mesoporous Silica or Carbon Frameworks after the Removal of Carbon or Silica[a]

	TEOS	resol	F127	polymer%[b]	SiO_2%[b]	C–H–O%[c]	SiO_2%[c]
MP-CS-27	2.08	0.16	1.0	34	66	27	73
MP-CS-36	2.08	0.5	1.0	42	58	36	64
MP-CS-46	2.08	1.0	1.6	51	49	46	54
MP-CS-61	2.08	2.0	2.3	68	32	61	39
MP-CS-36*	2.08	0.5	1.0	41	59	35	65
MP-CS-0	2.08		1.0	0	100	0	100
MP-CS-100	0	1.0	1.0	100	0	100	0

[a] The mass ratio of TEOS/EtOH/HCl/H_2O was fixed at $2.08:12:7.3 \times 10^{-3}:1.0$. [b] Polymer% and SiO_2% were the mass percentages in the polymer−silica nanocomposites, determined from TG results. [c] C−H−O% and SiO_2% were the mass percentages in the carbon−silica nanocomposites, determined from TG results. The elemental analysis results show that the carbon materials after the removal of silica have a molar ratio C:H:O = 14.4:2.5:1. The data of MP-CS-100 (FDU-15) came from ref 21.

2.2. Preparation of Resol Precursors. The resol precursor (M_w < 500) was prepared according to the literature method.[21] In a typical procedure, 0.61 g of phenol was melted at 40−42 °C in a flask and mixed with 0.13 g of 20 wt % NaOH aqueous solution under stirring. After 10 min, 1.05 g of formalin (37 wt % formaldehyde) was added dropwise below 50 °C. Upon further stirring for 1 h at 70−75 °C, the mixture was cooled to room temperature and the pH value was adjusted to about 7.0 by HCl solution. After water was removed by vacuum evaporation below 50 °C, the final product was dissolved in ethanol (20 wt % ethanolic solution).

2.3. Synthesis of Ordered Mesoporous Polymer−Silica and Carbon−Silica Nanocomposites. Mesoporous polymer−silica and carbon−silica nanocomposites were prepared by triconstituent co-assembly of resols, oligomer silicates from TEOS, and triblock copolymer F127 template. In a typical preparation, 1.6 g of block copolymer F127 was dissolved in 8.0 g of ethanol with 1.0 g of 0.2 M HCl and stirred for 1 h at 40 °C to afford a clear solution. Next, 2.08 g of TEOS and 5.0 g of 20 wt % resols' ethanolic solution were added in sequence. After being stirred for 2 h, the mixture was transferred into dishes. It took 5−8 h at room temperature to evaporate ethanol and 24 h at 100 °C in an oven to thermopolymerize. The as-made products, flaxen and transparent films or membranes, were scraped from the dishes and ground into fine powders. Calcination was carried out in a tubular furnace at 350 °C for 3 h and at 900 °C for 2 h under N_2 flow to get mesoporous polymer−silica and carbon−silica nanocomposites, respectively, named as MP-CS-46. "MP-CS-*x*" denotes the mesoporous polymer−silica and carbon−silica nanocomposite samples, wherein *x* represents the percentage of the carbon-compound content in the carbon−silica nanocomposite after 900 °C calcination. The heating rate was 1 °C/min below 600 °C and 5 °C/min above 600 °C. Nanocomposites with different compositions (the mass ratios of polymer/SiO_2 or C/SiO_2 from zero to infinity) could be synthesized by adjusting the mass ratios of resol to TEOS from zero to infinity (Table 1). To keep the initial silica oligomers at the same degree of hydrolysis and condensation, the mass ratio of TEOS/EtOH/HCl/H_2O was fixed at $2.08:12:7.3 \times 10^{-3}:1.0$. According to the different amounts of resol and F127, the final compositions were F127/resol/TEOS/EtOH/HCl/H_2O = $1-2.3:0.16-2:2.08:12:7.3 \times 10^{-3}:1.0$ (mass ratio). The typical samples denoted as MP-CS-27, -36, -46, and -61 are listed in Table 1.

Using the same initial composition as MP-CS-36 (F127/resol/TEOS/EtOH/HCl/H_2O = $1:0.5:2.08:12:7.3 \times 10^{-3}:1.0$ in mass ratio), nanocomposite MP-CS-36* was prepared by prolonging the stirring time to 5 h at 40 °C. In a typical preparation, 1.0 g of block copolymer F127, 10.0 g of ethanol, and 1.0 g of 0.2 M HCl were mixed well at 40 °C. To it were added 2.08 g of TEOS and 2.5 g of 20 wt % resol solution, and stirring was continued for 5 h. The following procedures were the same as the above description.

2.4. Synthesis of Ordered Mesoporous Carbon and Silica from Carbon−Silica Nanocomposites. After carbon−silica nanocomposites were immersed in 10 wt % HF solutions for 24 h, silicas were removed and mesoporous carbons were left. Calcination at 550 °C for 5 h in air could burn off carbons and generate mesoporous silica materials. The mesoporous pure carbon products were named as MP-C-27, -36, -46, and -61, respectively, and the mesoporous pure silica products were named as MP-S-27, -36, -46, and -61, respectively, corresponding to their mother nanocomposites.

2.5. Synthesis of FDU-15 Mesoporous Polymer and Carbon. FDU-15 samples with carbon-compound content percentage of 100% (MP-CS-100) were synthesized by a solvent evaporation-induced self-assembly (EISA) method with copolymer F127 as a template in an ethanol solution.[21] In a typical preparation, 1.0 g of F127 was dissolved in 20.0 g of ethanol, and then 5.0 g of 20 wt % resols' ethanolic solution was added by stirring for 10 min to form a homogeneous solution. The following procedures were the same as those for MP-CS-46. The as-made products were calcined at 350 and 900 °C in N_2 to get FDU-15 and C-FDU-15, respectively.

2.6. Characterization and Measurements. The small-angle X-ray scattering (SAXS) measurements were taken on a Nanostar U small-angle X-ray scattering system (Bruker, Germany) using Cu Kα radiation (40 kV, 35 mA). The *d*-spacing values were calculated by the formula $d = 2\pi/q$, and the unit cell parameters were calculated from the formula $a = 2d_{10}/\sqrt{3}$. X-ray diffraction (XRD) patterns were recorded on a Bruker D4 X-ray diffractometer with Ni-filtered Cu Kα radiation (40 kV, 40 mA). Nitrogen sorption isotherms were measured at 77 K with a Micromeritcs Tristar 3000 analyzer. Before measurements, the samples were degassed in a vacuum at 200 °C for at least 6 h. The Brunauer−Emmett−Teller (BET) method was utilized to calculate the specific surface areas (S_{BET}) using adsorption data in a relative pressure range from 0.04 to 0.2. By using the Barrett−Joyner−Halenda (BJH) model, the pore volumes and pore size distributions were derived from the adsorption branches of isotherms, and the total pore volumes (V_t) were estimated from the adsorbed amount at a relative pressure P/P_0 of 0.992. The micropore volumes (V_m) and micropore surface areas (S_m) were calculated from the $V-t$ plot method using the equation $V_m/cm^3 = 0.001547I$, where *I* represents the *y* intercepts in the $V-t$ plots. The *t* values were calculated as a function of the relative pressure using the de Bore equation, $t/Å = [13.99/(\log(p_0/p) + 0.0340)]^{1/2}$. Transmission electron microscopy (TEM) experiments were conduced on a JEOL 2011 microscope (Japan) operated at 200 kV. The samples for TEM measurements were suspended in ethanol and supported onto a holey carbon film on a Cu grid. Fourier transform infrared (FT-IR) spectra were collected on Nicolet Fourier spectrophotometer, using KBr pellets of the solid samples. Weight changes of the products were monitored using a Mettler Toledo TGA-SDTA851 analyzer (Switzerland) from 25 to 900 °C under nitrogen or air with a heating rate of 5 °C/min. ^{13}C and ^{29}Si solid-state nuclear magnetic resonance (NMR) experiments were performed on a Bruker DSX300 spectrometer (Germany) under conditions of cross polarization (CP) and magic angle sample spinning (MAS). ^{13}C CP-MAS NMR spectra were collected at room temperature with a frequency of 75 MHz (2 s recycle, 2.5 ms contact time) using adamantane as a reference. ^{29}Si solid-state MAS NMR spectra were collected at room temperature with a frequency of 59.6 MHz, a recycling delay of 600 s, a radiation frequency intensity of 62.5 kHz, and a reference sample of Q_8M_8 ($[(CH_3)_3SiO]_8Si_8O_{12}$). Raman spectra were obtained with a Dilor LabRam-1B microscopic Raman spectrometer (France), using a He−Ne laser with an excitation wavelength of 632.8 nm. The C, H, and O contents were measured on a Vario EL III elemental analyzer (Germany). Before the measurements, the silica components were removed from polymer−silica or carbon−silica nanocomposites.

Table 2. Physicochemical Properties of the Mesoporous Polymer−Silica and Carbon−Silica Nanocomposites Prepared with Different Resol/TEOS Mass Ratios from Triconstituent Co-assembly via EISA Method, and of the Corresponding Mesoporous Silica and Carbon Frameworks Obtained after the Removal of Carbon and Silica, Respectively[a]

sample name		a_0 (nm)	S_{BET} (m^2/g)	D (nm)	V (cm^3/g)
MP-CS-27	as-made	16.0			
	polymer−silica	12.6	600	8.5	0.65
	carbon−silica	7.79	160	6.7	0.21
MP-C-27	carbon		1270	0	0.73
MP-S-27	silica	12.0	240	7.8	0.40
MP-CS-36	as-made	14.8			
	polymer−silica	13.9	570	7.5	0.60
	carbon−silica	12.2	290	6.6	0.28
MP-C-36	carbon	11.7	2470	5.8	2.02
MP-S-36	silica	11.4	310	7.9	0.55
MP-CS-46	as-made	15.0			
	polymer−silica	13.4	610	8.1	0.80
	carbon−silica	12.0	350	6.7	0.46
MP-C-46	carbon	11.9	2390	6.7	1.94
MP-C-46	silica	10.8	270	10.7	0.79
MP-CS-61	as-made	15.6			
	polymer−silica	13.6	590	7.4	0.72
	carbon−silica	11.6	460	6.0	0.57
MP-C-61	carbon	11.6	1600	6.0	1.22
MP-S-61	silica	9.1	280	9.6	0.75
MP-CS-36*	as-made	14.8			
	polymer−silica	13.7	550	7.6	0.57
	carbon−silica	12.1	280	6.3	0.38
MP-C-36*	carbon	11.7	2130	2.6/5.8	2.02
MP-S-36*	silica	11.6	360	7.3	0.71
MP-CS-0	as-made	15.5			
	silica-550	12.6	230	6.5	0.32
	silica-900	11.4	60	4.4	0.07
MP-CS-100	as-made	14.8			
FDU-15	polymers	12.1	650	6.8	0.63
C-FDU-15	carbon	8.7	970	2.9	0.56

[a] The data of MP-CS-100 (FDU-15) came from ref 21. a_0, the unit cell parameter, was calculated by using the formula $a_0 = 2d/\sqrt{3}$. S_{BET} is the BET surface area. D is the pore size diameter. V is the total pore volume.

3. Results and Discussion

3.1. Ordered Mesostructured Polymer−Silica and Carbon−Silica Nanocomposites. Mesostructured polymer−silica nanocomposites were prepared by triconstituent co-assembly of preformed resols, silica oligomers from acid-catalyzed hydrolysis of TEOS, and triblock copolymers F127 via the EISA approach[28] in ethanol solution. Here, we take the mesoporous nanocomposite MP-CS-46 with the carbon-compound content percentage of 46 wt % as an example. The as-made products are flaxen membranes without obvious macrophase separation. The SAXS pattern for as-made polymer−silica nanocomposite MP-CS-46 (Supporting Information, Figure 1a) clearly shows three well-resolved diffraction peaks, associated with 10, 11, and 20 reflections of two-dimensional (2-D) hexagonal symmetry with the space group of *p*6*m*.[29] After calcination at 350 °C in nitrogen, the product turns brown and yields a more resolved SAXS pattern (Supporting Information, Figure 1b) of highly ordered 2-D hexagonal mesostructure. The unit cell parameter (a_0) is reduced from 15.0 to 13.4 nm upon the calcination (Table 2), reflecting a 10.7% framework shrinkage. After being heated at 900 °C in nitrogen, the nanocomposite

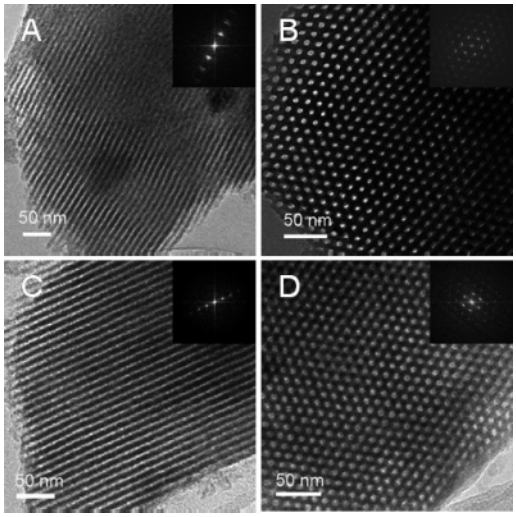

Figure 1. TEM images of mesoporous nanocomposites MP-CS-46 calcined at 350 °C (A and B) and 900 °C (C and D) in N_2, viewed from the [110] (A and C) and [001] (B and D) directions. The insets are the corresponding FFT diffractograms.

becomes black. Besides three well-resolved diffraction peaks indexed to 10, 11, and 20 reflections, an additional weak diffraction peak indexed to 21 reflection is observed (Supporting Information, Figure 1c), indicating that highly ordered 2-D hexagonal mesostructured nanocomposite is thermally stable. The unit cell parameter (a_0) is calculated to be 12.0 nm, reflecting minor framework shrinkage of 20%. It is much smaller than that of C-FDU-15 (41.2%) with the same *p*6*m* symmetry but without silicates inside the framework after heating treatment at 900 °C. This phenomenon clearly demonstrates that the presence of silica in the nanocomposite can efficiently reduce framework shrinkage as compared to pure polymer.[27]

A more detailed structural characterization is revealed by TEM images, as shown in Figure 1. The calcined nanocomposites at 350 and 900 °C in N_2 show large domains of highly ordered stripe-like and hexagonally arranged images. The results indicate well-ordered hexagonal arrays of mesopores with 1-D channels,[29] which can be retained after calcination at 900 °C. It further confirms a thermally stable *p*6*m* mesostructure. Estimated from TEM images, the cell parameters (a_0) are 13.2 and 12.0 nm for the nanocomposites calcined at 350 and 900 °C, respectively, in accordance with the values calculated from SAXS data.

N_2 sorption isotherms of this mesoporous nanocomposite (MP-CS-46) calcined at 350 °C in N_2 (Supporting Information, Figure 2) exhibit type-IV curves with a very sharp capillary condensation step at $P/P_0 = 0.70-0.80$ and an H_1-type hysteresis loop that are typical of large-pore mesoporous materials with cylindrical channels.[29] A narrow pore size distribution with a mean value of 8.1 nm is calculated from the adsorption branch based on the BJH model. It is a little larger than the pore size (6.8 nm) of FDU-15 (Table 2),[21] indicative of a smaller framework shrinkage of the nanocomposite during thermal decomposition of triblock copolymer F127 than the latter case. This phenomenon is coincident with the SAXS results. The polymer−silica nanocomposite (MP-CS-46) has a BET surface area of 610 m^2/g and a total pore volume of 0.80 cm^3/g, respectively.[21] *t*-Plot analysis (Supporting Information, Figure 3a) reveals the contribution of micropores to the BET surface area is about 17.2%. After calcination at 900 °C in N_2,

(28) Lu, Y. F.; Ganguli, R.; Drewien, C. A.; Anderson, M. T.; Brinker, C. J.; Gong, W. L.; Guo, Y. X.; Soyez, H.; Dunn, B.; Huang, M. H.; Zink, J. I. *Nature* **1997**, *389*, 364.
(29) Zhao, D. Y.; Feng, J. L.; Huo, Q. S.; Melosh, N.; Fredrickson, G. H.; Chmelka, B. F.; Stucky, G. D. *Science* **1998**, *279*, 548.

this nanocomposite MP-CS-46 with 46 wt % carbon-compound content also displays type-IV N_2 sorption isotherms but with an H_2-type hysteresis loop. It is related to imperfect cylinder channels,[30] implying the presence of a rough surface probably caused by asymmetric shrinkage. The capillary condensation step shifts to low relative pressure with a wide range of $P/P_0 = 0.45-0.67$, which is related to the reduction of pore size to 6.7 nm. This phenomenon is accompanied by the change of cell-unit parameters on account of framework shrinkage during the calcination. As compared to the distinct decrease of pore size to 2.9 nm for C-FDU-15 with 100% carbon content heated at 900 °C in N_2 (Table 2), this shrinkage in the nanocomposite is considerably smaller. The BET surface area and pore volume of the MP-CS-46 nanocomposite calcined at 900 °C are calculated to be 350 m^2/g and 0.46 cm^3/g, respectively.

Efforts were then made to elucidate the framework compositions by the combination of TGA, FT-IR, NMR spectra, and elemental analyses. TGA curves (Supporting Information, Figure 4A) show a significant weight loss of 46 wt % in the temperature range from 300 to 400 °C under nitrogen for as-made nanocomposite MP-CS-46. Similarly, 97.5 wt % loss of pure triblock copolymer F127 occurs at the same temperature range. It suggests that most F127 template can be removed at 350 °C in N_2. A little weight loss (10 wt %) can be observed at 400−900 °C, corresponding to dehydrogenation and polymerization of phenolic resins and silicate species in the nanocomposite. Beginning with the nanocomposite MP-CS-46 after calcination at 350 °C in N_2, the TGA curve (Supporting Information, Figure 4B) displays an obvious weight loss of 51 wt % in air between 350 and 580 °C. This phenomenon is attributed to the combustion of organic constituents with residue of inorganic constituent silicates. The composition can then be given as organics of 51 wt % and silica of 49 wt % as listed in Table 1. It may fluctuate a bit because condensation of silicate species may also contribute to the weight loss.[29] When TGA measurement was carried out on MP-CS-46 after calcination at 900 °C in N_2, the weight loss in the temperature range of 500−600 °C is 46 wt %, and the weight residue is 54 wt %. They are attributed to carbon compound and silica, respectively.

FT-IR spectra (Supporting Information, Figure 5a) of as-made nanocomposite MP-CS-46 show the bands at ∼2900 and 1100 cm^{-1} attributed to the C−H and C−O stretching of triblock copolymer F127[31] and the overlap with Si−O−Si vibration.[32] A broad band at ∼3400 cm^{-1} and weak band at 1610 cm^{-1} assigned to the characteristic stretching modes of phenolic resins[33,34] and the absorbance at 942 cm^{-1} ascribed to Si−OH vibration are observed. The decreasing intensity of bands at around 2900 cm^{-1} for the nanocomposite calcined at 350 °C under nitrogen further suggests template decomposition of copolymer F127.[31] The retained vibrations of phenolic resins and silicates indicate the coexistence of polymer and inorganic silicate solids. To obtain the composition of organic materials, silicates were etched by HF solution. Elemental analysis reveals that it is composed of C, 51.3 wt %; H, 3.2 wt %; and O, 10.1 wt %, the molar ratio of C:H:O (6.77:5.03:1) close to that in ideal cross-linking phenolic resins (C:H:O = 7:5:). It indicates that highly cross-linking phenol resin polymer networks are preserved well. The ^{13}C CP-MAS NMR spectrum (Figure 2A(a)) of as-made polymer−silica nanocomposite shows a strong resonance signal at 71 ppm, which is contributed by triblock copolymer F127.[35] Heated at 350 °C in nitrogen, the nanocomposite shows five peaks at the chemical shifts at 16, 35, 64, 130, and 149 ppm (Figure 2A(b)). Except for the weak signal at ∼64 ppm related to Si−O−C bonds, other signals are typical features of polymer phenolic resins, revealing the presence of resin polymeric frameworks in the nanocomposite and silicate surface partly bonding with carbon species.[36] No signal ascribed to Si−C bonds is detected. It gives a hint for only silica and polymer dispersing in the frameworks and no Si−C chemical bonds between them. The signal at 71 ppm corresponding to triblock copolymer F127 disappears after the calcination at 350 °C (Figure 2A(b)), which gives evidence on almost complete decomposition of triblock copolymer template in agreement with TG and FT-IR analyses.

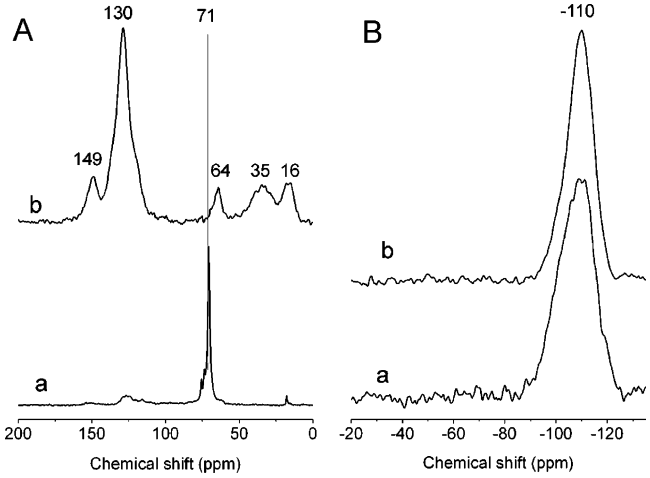

Figure 2. Solid-state ^{13}C CP/MAS NMR spectra (A) of mesoporous nanocomposites MP-CS-46: (a) as-made and (b) calcined at 350 °C in N_2. Solid-state ^{29}Si MAS NMR spectra (B) of mesoporous nanocomposites MP-CS-46: (a) calcined at 900 °C in N_2 and (b) after (a) burning at 550 °C in air.

After calcination at 900 °C in N_2, the characteristic vibration bands of phenolic resins disappear and those of silicates are retained as shown in FT-IR spectra (Supporting Information, Figure 5c−e), and the molar ratios of C:H:O estimated by elemental analysis increase to 14.4:2.5:1.0 after etching SiO_2 with HF. These results clearly indicate the framework is composed of carbon and silica. The ^{29}Si MAS NMR spectrum (Figure 2B(a)) of the nanocomposite MP-CS-46 calcined at 900 °C in N_2 shows a broad signal at −110 ppm, which is similar to the chemical shift of Q^4 species [O≡Si−O] for amorphous silica. The result illustrates that the silicate species with a complex chemical environment have relatively high cross-linking degree and some interactions with carbon species. No other chemical shift is detected at −60 ppm, suggesting that no Si−C species are formed in the nanocomposite.[7]

The ratios of polymer/silica or carbon/silica in the polymer−silica or carbon−silica nanocomposites can be tuned from zero

(30) Chen, D. H.; Li, Z.; Wan, Y.; Tu, X. J.; Shi, Y. F.; Chen, Z. X.; Shen, W.; Yu, C. Z.; Tu, B.; Zhao, D. Y. *J. Mater. Chem.* **2006**, *16*, 1511.
(31) Yang, C. M.; Zibrowius, B.; Schmidt, W.; Schuth, F. *Chem. Mater.* **2003**, *15*, 3739.
(32) Sun, D. H.; Zhang, R.; Liu, Z. M.; Huang, Y.; Wang, Y.; He, J.; Han, B. X.; Yang, G. Y. *Macromolecules* **2005**, *38*, 5617.
(33) Trick, K. A.; Saliba, T. E. *Carbon* **1995**, *33*, 1509.
(34) Kim, J.; Lee, J.; Hyeon, T. *Carbon* **2004**, *42*, 2711.
(35) Chu, P. P.; Wu, H. D. *Polymer* **2000**, *41*, 101.
(36) GrenierLoustalot, M. F.; Larroque, S.; Grenier, P. *Polymer* **1996**, *37*, 639.

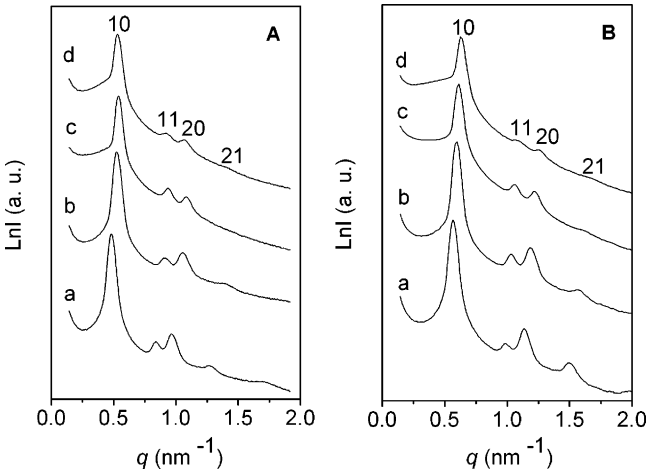

Figure 3. SAXS patterns of the mesoporous nanocomposites prepared with different compositions calcined at 350 °C (A) and 900 °C in N_2 (B). In both (A) and (B), (a) MP-CS-27, (b) MP-CS-36, (c) MP-CS-46, and (d) MP-CS-61.

to infinity by varying the mass ratios of resols to TEOS in triconstituent co-assembling process. To well organize triconstituent co-assembly and obtain highly ordered mesostructures, different amounts of resol and F127 are required in the system with the fixed mass ratios for TEOS:EtOH:HCl:H_2O of 2.08: 12:7.3 × 10^{-3}:1.0. The synthesis conditions and compositions for four typical nanocomposites with the carbon-compound contents (wt %) of 27, 36, 46, and 61, and two samples of MP-S-0 (pure silica) and MP-C-100 (pure polymer, FDU-15) with carbon-compound contents of 0 and 100%, respectively, as examples, are illuminated in Table 1. The four nanocomposites after calcination at 350 and 900 °C in N_2 show typical SAXS patterns of high-quality 2-D hexagonal mesostructure (Figure 3). At least three or four resolved diffraction peaks can be observed.[29] As carbon contents in the nanocomposites increase, the mesostructure regularity gradually reduces to some extent. These results also suggest that the mesoporous polymer−silica and carbon−silica nanocomposites are thermally stable. The unit cell parameters (Table 2) become smaller as compared to as-made nanocomposites because of the structural shrinkage. Notably, all unit parameters are much larger than that of FDU-15 or C-FDU-15, indicating that the incorporation of rigid inorganic silicates reduces framework shrinkage.[27] This effect also lies in the fact that polymer−silica and carbon−silica nanocomposites with more silicate contents have larger unit cell parameters (a_0).

N_2 sorption isotherms and pore size distribution curves of polymer−silica and carbon−silica nanocomposites with different carbon contents are shown in Figure 4, and the corresponding pore characters including BET surface areas, pore volumes, and pore diameters are summarized in Table 2. All nanocomposites exhibit type-IV curves with distinct capillary condensation steps, suggesting narrow mesopore size distributions.[29] It is coincident with their highly ordered mesostructures, confirmed by the SAXS and TEM results. When carbon contents are low, obvious H_2 hysteresis can be seen for the polymer−silica nanocomposites (Figure 4A(a,b)) after calcination at 350 °C in N_2, suggesting caged pore mesostructure. It further suggests that the nanocomposites have roughly cylindrical pore channels, probably resulting from the different shrinkage between silicates and phenolic polymer resins.[30] This implies local component non-

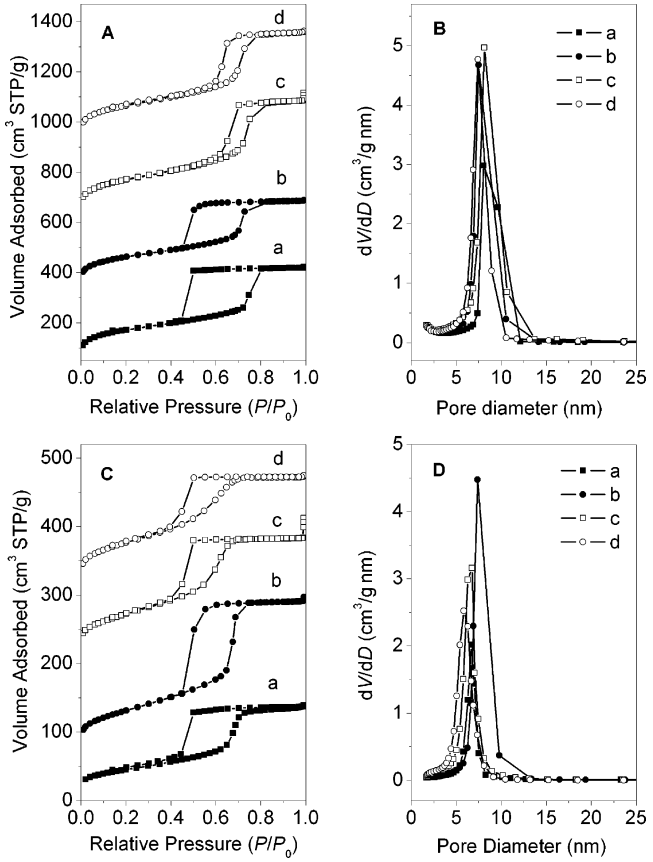

Figure 4. N_2 sorption isotherms (A and C) and pore size distribution curves (B and D) of the mesoporous nanocomposites calcined at 350 °C (A and B) and 900 °C in N_2 (C and D). In all figures, a, b, c, and d correspond to the polymer−silica and carbon−silica nanocomposites of MP-CS-27, MP-CS-36, MP-CS-46, and MP-CS-61, respectively. The isotherms (A) for MP-CS-36, MP-CS-46, and MP-CS-61 calcined at 350 °C in N_2 are offset vertically by 300, 600, and 900 cm^3/g, respectively. The isotherms (C) of MP-CS-36, MP-CS-46, and MP-CS-61 calcined at 900 °C in N_2 are offset vertically by 50, 180, and 250 cm^3/g, respectively.

uniformity. When carbon contents are high, ideal H_1 hysteresis can be observed for polymer−silica nanocomposites (Figure 4A(c,d)), suggesting well-ordered cylinder mesopore channels.[29] Polymer−silica nanocomposites have similar BET surface areas and uniform mean pore sizes regardless of carbon contents (Figure 4B). All carbon−silica nanocomposites after calcination at 900 °C in N_2 show H_2 hysteresis (Figure 4C), suggesting imperfect mesopore channels.[30] As carbon contents increase in carbon−silica nanocomposites, both BET surface areas and pore volumes gradually enlarge. Yet the mean pore sizes remain a value about 6.7 nm (Figure 4D and Table 2), which is greatly larger than that (2.9 nm) of C-FDU-15 with pure carbon framework. It implies that the framework shrinkage in the nanocomposite is considerably smaller.

It is noticed that triblock copolymer F127 self-assembly can derive either pure silica or polymer frameworks with ordered mesostructure. The dosage of F127 is different for various components. For example, pure polymer mesostructure (MP-CS-100) with 2-D hexagonal *p*6*m* symmetry, typical FDU-15, can be templated by copolymer F127 without the addition of silica source TEOS when the phenol/F127 mass ratio ranges from 1.0 to 1.2.[21] The highly ordered mesoporous silica structure with carbon-content percentage of zero can be obtained at the mass ratio of TEOS/F127 = 2.08 via the similar EISA process.

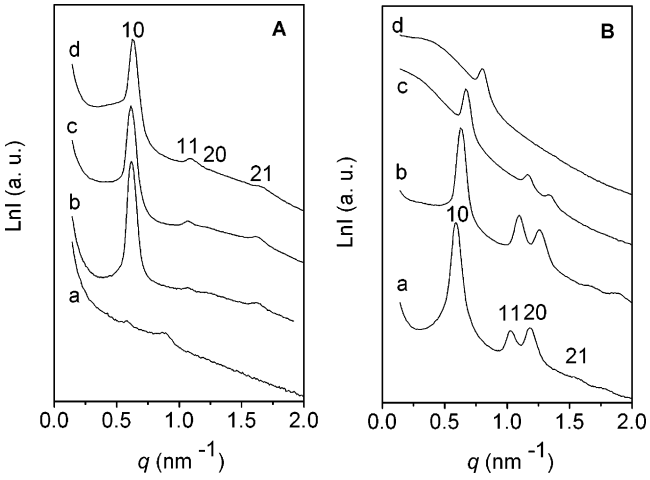

Figure 5. SAXS patterns of the mesoporous carbon (A) and silica (B) products obtained from the corresponding nanocomposites with different compositions calcined at 900 °C in N_2. In (A): (a) MP-C-27, (b) MP-C-36, (c) MP-C-46, and (d) MP-C-61. In (B): (a) MP-S-27, (b) MP-S-36, (c) MP-S-46, and (d) MP-S-61.

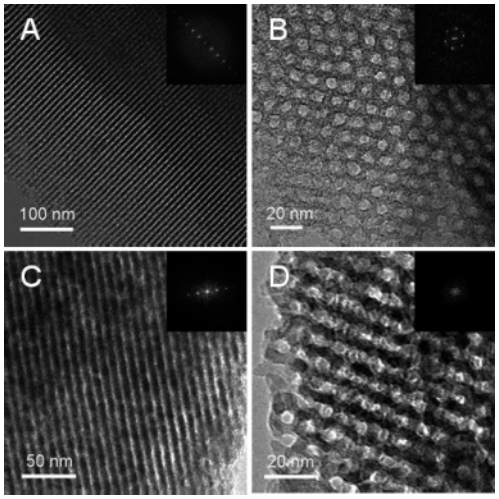

Figure 6. TEM images of the products from the MP-CS-46 nanocomposite calcined at 900 °C in N_2: mesoporous carbon MP-C-46 (A and B) and mesoporous silica MP-S-46 (C and D). The TEM images were recorded along the [110] (A and C) and [001] (B and D) directions. The insets are the corresponding FFT diffractograms.

Therefore, the polymer−silica mesostructure can probably have a constituent-ratio range from zero to infinity with the same *p*6*m* symmetry by controlling the amount of both precursors and triblock copolymer F127.

3.2. Ordered Mesoporous Carbon and Silica Materials from Carbon−Silica Nanocomposites. The integrated frameworks with ordered 2-D hexagonal mesostructure have been synthesized by triconstituent co-assembly via the one-step EISA approach, composed of silicas and polymer resins or silicas and carbons. Either polymer−silica or carbon−silica nanocomposites have a very wide component range. Some interactions may occur on the interface between the polymer and silica or carbon and silica, and affect the structures and networks. Yet no Si−C covalent bonds are formed. To understand the structures of carbon (polymer) and silica in the nanocomposites is critical for the control of triconstituent co-assembly, and thus it is necessary to investigate the resultants of carbon and silica separately. Carbon−silica nanocomposites are used as the parents. Etching with HF solution or combustion of nanocomposites in air can remove silica or carbon, leaving carbon or silica phases.

3.2.1. Ordered Mesoporous Carbon Materials. TG measurements (Supporting Information, Figure 4B) show that carbons can completely combust (∼99.7 wt %) in air at a temperature range from 400 to 600 °C. It indicates that silicas have been successfully removed from carbon−silica nanocomposites by dissolution in HF, which can also be confirmed by TEM-based energy-dispersive X-ray spectroscopy (EDS) analyses (not shown here). The SAXS patterns (Figure 5A) of all mesoporous carbon materials except that of MP-C-27 with low carbon content show three or four diffraction peaks, revealing ordered 2-D hexagonal mesostructure (*p*6*m*)[29] with similar unit cell parameters of about 12 nm. They are analogous to mother carbon−silica nanocomposites (Table 2). The small framework shrinkages are related to the mild aqueous treatment by HF solution rather than a serious heating treatment at high temperature. As compared to pure carbon C-FDU-15, these mesoporous carbons show remarkably larger unit cell parameters despite similar values for as-made nanocomposites and FDU-15. It can be attributed to the inhibition of framework shrinkages by the presence of silicas in nanocomposites during carbonization. Representative TEM images of the mesoporous carbon MP-C-46 which was derived from mother nanocomposite MP-CS-46 viewed from the [110] and [001] directions, respectively (Figure 6A,B), further confirm a highly ordered 2-D hexagonal *p*6*m* mesostructure.[29] The cell parameter (a_0) is estimated to be 11.8 nm, in good agreement with that determined from the SAXS data. Carbon obtained from MP-CS-27 lacks well-resolved SAXS patterns (Figure 5A(a)), indicative of a disordered mesostructure. It can be ascribed to the low carbon content in the nanocomposites, which may leave many voids. Ordered mesostructure cannot be retained after the removal of silica. From this point, ordered mesoporous carbon materials can be derived provided that the carbon contents are higher than 35 wt % in mesoporous carbon−silica nanocomposites.

N_2 sorption isotherms were measured on the mesoporous carbon materials to evaluate their textural properties, as shown in Figure 7A,B and Table 2. Mesoporous carbons except the carbon product from MP-CS-27 exhibit similar type-IV isotherms with distinct capillary condensation steps occurring at relative pressures of 0.6−0.7, corresponding to narrow pore size distributions of mesopores at about 6 nm.[29] Yet the mean pore sizes remain a value about 6.7 nm (Table 2). The pore sizes are close to those of their mother nanocomposites. These mesopores are, therefore, inherited from carbon−silica nanocomposites due to the degradation of triblock copolymer F127 and can retain comparative large values due to small contraction.

Remarkably, a distinctly increased sorption in the isotherm curves at relative pressure of P/P_0 of 0.1−0.3 is observed for mesoporous carbons (Figure 7A), suggesting smaller pores with a wide distribution below 3.5 nm (Figure 7B). The smaller pores are inside the pore walls caused by the removal of silicas from the carbon-silica composites. It implies that carbon and silica phases are separated and "homogeneously" distributed inside pore walls on nanoscale. Another distinguished phenomenon is extremely high BET surface areas of about 2400 m^2/g for the mesoporous carbons MP-C-36 and MP-C-46, almost 7 times higher than their parent carbon−silica nanocomposites (Table 2). On the basis of an ideal cylinder model, the calculated BET

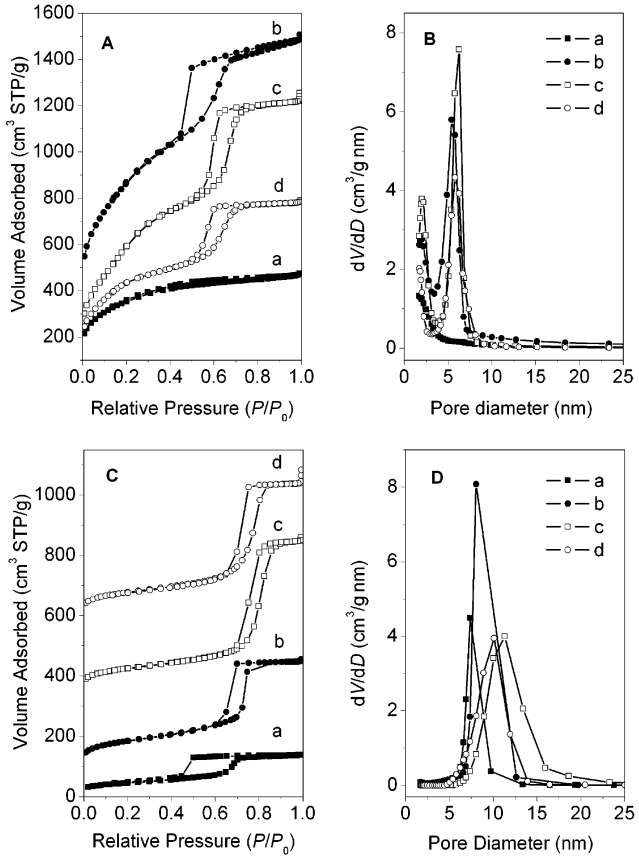

Figure 7. N_2 sorption isotherms (A and C) and pore size distribution curves (B and D) of the mesoporous carbon (A and B) and silica (C and D) products from the mother nanocomposites with different compositions calcined at 900 °C in N_2. In all figures, a, b, c, and d correspond to the carbon and silica products from MP-CS-27, MP-CS-36, MP-CS-46, and MP-CS-61, respectively. The isotherms (A) for the mesoporous carbon MP-C-46 are offset vertically by 200 cm^3/g, and those (C) for mesoporous silicas MP-S-36, MP-S-46, and MP-S-61 are offset vertically by 100, 300, and 600 cm^3/g, respectively.

surface area is only 350 m^2/g when the density of carbon framework is assumed to be 1.8 g/cm^3. The large surface areas may be ascribed from plenty of small pores inside carbon pore walls. Carbon from nanocomposite MP-CS-61 whose mother has a low content of 39 wt % silica shows a lower BET surface area of 1600 m^2/g, possibly due to less small pores. This kind of carbon completely differs from the reported C-FDU-15 obtained without silica whose surface areas are mainly contributed by micropores.[21] The isotherms of mesoporous carbon MP-C-27 obtained from low carbon-content nanocomposite MP-CS-27 show type-I curves with a wide pore distribution of less than 2.5 nm (Figure 7A(a) and B(a)). MP-C-27 has a BET surface area of 1270 m^2/g. It is probably contributed by the dissolution of silica in the carbon−silica nanocomposite, although the mesostructure of MP-C-27 is destroyed after etching silica.

The wide-angle XRD pattern (Supporting Information, Figure 6) for mesoporous carbons shows a weak diffraction shoulder at 2θ of about 23°, together with a broad diffraction peak at 2θ value of about 43°, corresponding to 002 and 10 reflections of carbon materials.[37,38] Raman spectrum (Supporting Information, Figure 7) displays two broad peaks at around 1330 and 1600 cm^{-1}, attributed to the D-band and G-band, respectively.[38] These results give evidence for amorphous carbon frameworks, which may be related to the carbon precursors of phenolic resins and the low calcination temperature.[19]

3.2.2. Ordered Mesoporous Silica Materials. Burning carbon−silica nanocomposites in air at 550 °C brings about the corresponding ordered mesoporous silica materials, as evidenced by characteristics of well-resolved SAXS patterns (Figure 5B) and typical TEM images (Figure 6C and D) with 2-D hexagonal *p6m* symmetry.[29] On the contrary to the nearly constant unit cell parameters of both ordered mesoporous carbons and carbon−silica nanocomposites, the unit cell parameters of ordered mesoporous silicas gradually reduce as carbon contents increase in their mother nanocomposites (Figure 5B and Table 2). This phenomenon can be explained by the increasing framework shrinkage during the combustion at 550 °C in air with the continuous augment of carbon contents in the nanocomposites. Interconnected channels of mesoporous silica, for the mesoporous silica from MP-CS-46, can be clearly observed from the TEM image (Figure 6D). It may be attributed to the destruction of nanocarbon internets during the carbon combustion, similar to 3D-SBA-15.[39] For the mesoporous silica from MP-CS-61 with carbon content as high as 61 wt %, only one weak diffraction peak can be detected in the SAXS pattern (Figure 5B(d)). There are two possible reasons. One is that the silica mesostructure has been destroyed during a large amount of carbon combustion, similar to the carbon mesostructure whose mother nanocomposites have a high content of silica. The other may be a low contrast for X-ray diffraction due to voids caused by copious carbon combustion and small residue of silica.

Type-IV N_2 sorption isotherms with capillary condensation steps at a relative pressure of 0.70−0.85 are observed for all mesoporous silica materials derived from carbon−silica nanocomposites by simple combustion at 550 °C in air (Figure 7C), suggesting a uniform pore size distribution. On comparison with their mother carbon−silica nanocomposites, the pore sizes calculated from adsorption branches for ordered mesoporous silicas are a little larger (Table 2), and their distributions get wider (Figure 7D). The pore sizes of carbons whose mother nanocomposites have high-content carbons, for example, MP-CS-46 and MP-CS-61, are visibly larger than the corresponding a_0 values. It is not surprising because similar phenomenon has been observed in meso-tunneled 3D-SBA-15.[39] Two effects can be considered on the enlargement of pore sizes, the minor one of inner-wall carbon combustion and the major one of large mesopore tunnels (>4 nm) on pore walls as observed by the TEM image (Figure 6D). The large enough meso-tunnels together with uniform cylinder channels contribute the space for nitrogen condensation at higher relative pressure (P/P_0), reflecting a larger calculated pore size. Simultaneously, the wide pore size distributions support the conclusion. These mesoporous silica materials have BET specific surface areas and pore volumes ranging from 240 to 310 m^2/g and from 0.40 to 0.79 cm^3/g (Table 2), respectively, which are much lower than their mesoporous carbon counterparts. The solid-state ^{29}Si-MAS NMR spectrum (Figure 2B(b)) for mesoporous pure silica (MP-S-46) calcined at 550 °C in air shows a narrower signal at −110

(37) Hoebbel, D.; Nacken, M.; Schmidt, H. *J. Sol.-Gel Sci. Technol.* **1998**, *12*, 169.
(38) Yang, H. F.; Yan, Y.; Liu, Y.; Zhang, F. Q.; Zhang, R. Y.; Meng, Y.; Li, M.; Xie, S. H.; Tu, B.; Zhao, D. Y. *J. Phys. Chem. B* **2004**, *108*, 17320.
(39) Fan, J.; Yu, C. Z.; Wang, L. M.; Tu, B.; Zhao, D. Y.; Sakamoto, Y.; Terasaki, O. *J. Am. Chem. Soc.* **2001**, *123*, 12113.

Scheme 1. Triconstituent Co-assembly to Ordered Mesoporous Polymer−Silica and Carbon−Silica Nanocomposites, and the Corresponding Ordered Mesoporous Silica and Carbon Frameworks

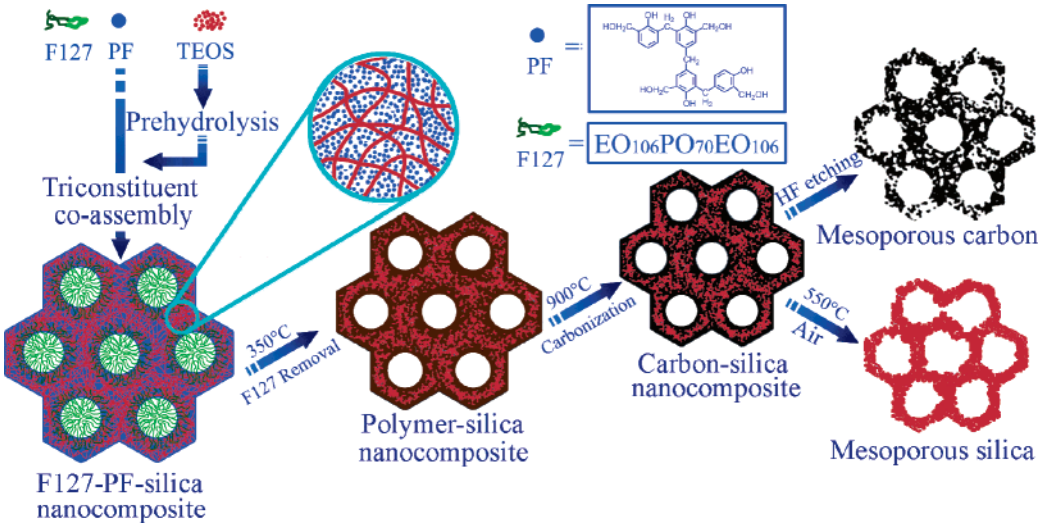

ppm (Q^4) than that for carbon−silica nanocomposite MP-CS-46 (Figure 2B(a)), implying an increase in the polymerization degree of silicates. The low BET surface areas may be related to the preparation method. Ordered mesoporous carbons were obtained by a mild dissolution of the silica in an aqueous HF solution without any further calcination. On the contrary, the removal of carbon in carbon−silica nanocomposite was rigorous by calcination at 550 °C in air. It may eliminate the small pores in silica walls left by removal of carbons and condense silica frameworks.

3.3. Understanding the Controllable Triconstituent Co-assembly. On the basis of the above observations, we propose that the formation of nanocomposites undergoes a triconstituent co-assembly process of organic polymer resol precursors, silicate oligomers hydrolyzed from TEOS, and amphiphilic triblock copolymer F127. The final nanocomposites have an interpenetrating framework with "reinforced-concrete"-like structure, in which both "reinforcing-steel-bar" silicate and "concrete" polymer resins or carbons can form mesostructured frameworks with nanoscaled phase separation (Scheme 1).

First, it is well known that TEOS or oligomer silicate species can react with the hydroxyl group of phenol or phenolic resins. Yet Si−O−C bonds are unstable as compared to Si−O−Si and C−C bonds individually formed during the polymerization process of resols and silicate oligomers. In our case, silicates and polymer resins or carbons are the two separated and coexisted constituents. Only a weak bonding interaction occurs between silicate surface and carbon species, but no Si−C species are formed in the nanocomposites. More importantly, both ordered mesoporous polymer resin (or carbon) and silica frameworks instead of scattered nanoparticles or nanowires can be derived from homogeneous polymer−silica nanocomposites. Because both of the individual frameworks can be obtained by the surfactant self-assembly approach, we can preliminarily separate them at the beginning of the assembly. It should be noted, however, that this separation is only for simplifying the understanding on co-assembly of polymers and silicates and surfactant F127. In fact, during the process of co-assembling inorganic and organic precursors into the desired surfactant−polymer−silica nanocomposites, there is a complicated balance between competition and cooperation among the inorganic−inorganic (silicate−silicate), organic−inorganic (F127−silicate and resol−silicate), and organic−organic (F127−F127, F127−resol, and resol−resol) interactions. As mentioned above, the used amount of surfactant F127 is varied to obtain highly ordered mesostructured materials when the mass ratio of the inorganic silicate to organic resol precursor ranges from zero to infinity. It is not a simple function, probably on account of the different amounts of hydroxyl groups in resol and silicate precursors.

To match well the triconstituent co-assembly system, resols and silicate oligomers from acid-catalyzed hydrolysis of TEOS are used as organic and inorganic precursors, respectively. This kind of resol that is preformed by phenol and formaldehyde under an alkaline condition has a 3-D network structure with benzene ring as three- or four-linking sites.[40] In the initial acid-hydrolyzed TEOS solution, small oligomers full of Si−OH groups are formed.[41] Both of them possess plenty of hydroxyl groups, which can form strong hydrogen-bonding interactions with EO-containing triblock polymers and are arranged around triblock copolymer micelles. Triblock copolymer F127 ($EO_{106}PO_{70}EO_{106}$) was selected as a template, mainly due to its long EO chains, which can form strong hydrogen-bonding interactions and favor the organization of ordered nanocomposite mesostructures.

The continuous ethanol evaporation promotes co-assembly of these species and drives the organization of surfactant−resols−silica composites into ordered liquid-crystalline mesophase.[42,43] The ordered mesophase is solidified, and a nanocomposite with ordered mesostructure can be obtained. During this process, resols show low condensation rates under acidic condition at room temperature and phase separation for organic species, and form nanosized "concrete" structures in the nanocomposites. However, silicate oligomers undergo a cooperative process, during which they not only assemble with the surfactants, but also condense and cross-link together to form

(40) Knop, A. P. L. A. *Phenolic Resins*; Springer: Berlin, 1985.
(41) Brinker, C. J.; Scherer, G. W. *Sol−Gel Science*; Academic Press: New York, 1990.
(42) Grosso, D.; Cagnol, F.; Soler-Illia, G.; Crepaldi, E. L.; Amenitsch, H.; Brunet-Bruneau, A.; Bourgeois, A.; Sanchez, C. *Adv. Funct. Mater.* **2004**, *14*, 309.
(43) Wan, Y.; Yang, H. F.; Zhao, D. Y. *Acc. Chem. Res.* **2006**, *39*, 423.

the frameworks. Because of the tetrahedral structures, the cross-linkage of silicate species can occur around nanosized resols to generate 3-D "reinforcing-steel-bar" frameworks. Therefore, the controllable triconstituent co-assembly of surfactants, resols, and silica species can be achieved with "homogeneous" distribution of resols and silicates around triblock copolymer F127 template. Large domain sized polymer resin "concrete" frameworks interpenetrated with silicate networks shape during the thermopolymerization of resols at 100 °C inside the framework mesostructure. Although a layered framework similar to graphite structure but quite different from silicate structure is the normal product of resol polymerization, inorganic silicates and polymer resins can coexist in a well-ordered, long-range architecture by local micro-phase separation.

Ordered mesoporous polymer−silica nanocomposites are obtained after the removal of the triblock copolymer template by calcination at 350 °C in N_2 flow. Upon the heating process at 900 °C in N_2, "concrete" polymers transform to carbons in high-quality mesoporous carbon−silica nanocomposites. Two constituents, polymer resins and silicates or carbons and silicates with the mass C/SiO_2 ratios ranging from zero to infinity, are "homogeneously" aggregated and dispersed in the frameworks on nanoscale with "reinforced-concrete" structures. The presence of "reinforcing-steel-bar" silicates in nanocomposites greatly inhibits framework shrinkage, yielding large-pore carbon−silica nanocomposites.

After a mild dissolution of silica in an aqueous HF solution, highly ordered mesoporous carbon frameworks can be obtained. They possess two kinds of pores. The primary pore diameter is determined by the size of the hexagonal arranged micelles that are co-assembled with organic surfactant molecules, resols, and silica oligomers. This kind of pore is large and almost similar to that of carbon−silica nanocomposites (Table 2). The others are small pores in the carbon walls caused by etching of silica frameworks. Because of the 3-D "reinforcing-steel-bar" framework of silicas, the pores on the "concrete" carbon walls are quite small (<2.5 nm). In contrast with C-FUD-15 heated at 900 °C,[21] this kind of mesoporous carbons shows considerably larger pore sizes of about 6.7 nm and higher surface areas up to 2470 m^2/g. Calcination at 550 °C in air can burn out carbon in carbon−silica nanocomposites, leaving ordered mesoporous silicas. Because of the elimination of "concrete" carbons, the mesostructures shrink and pore sizes enlarge to a small degree. Different from the removal of silicate "steel-bar" frameworks, the combustion of large sized "concrete" carbons leaves large disordered voids on silica frameworks. It results in large mesopore tunnels (>4 nm), and the pore sizes are sometimes even larger than the unit cell parameters (a_0).

Therefore, the initial hydrolysis and condensation degree of organic and inorganic precursors can be adjusted to obtain different domain-sized nanocomposites. It offers an opportunity to actually control the co-assembly from the viewpoints of not only the constituent distribution but also the structural and textual properties. On the basis of sol−gel chemistry,[41] prolonging the aging time of TEOS under HCl acid-catalyzed condition increases the polymerization and cross-linking degree of silicates. The nanocomposite MP-CS-36* was synthesized by stirring resols and TEOS under acidic ethanol solution for 5 h in the presence of triblock copolymer F127, with the same compositions as sample MP-CS-36. Almost no changes are found between the two carbon−silica nanocomposites and two mesoporous silica materials after the carbon combustion, suggested by SAXS, TEM, and nitrogen sorption techniques (Figures 8−10 and Table 2). The mesoporous silica from MP-CS-36* exhibits a smaller pore size (7.3 nm) than that (7.9 nm) of the silica from MP-CS-36, possibly due to more condensed silicate frameworks. Distinct variation is observed in two derived mesoporous carbon materials after etching silica, although they have the same ordered 2-D hexagonal mesostructure and amorphous frameworks as evidenced by the SAXS patterns (Figure 3B(b) and Figure 8a), wide angle XRD patterns (Supporting Information, Figure 6), Raman spectra (Supporting Information, Figure 7), and high-resolution TEM (HRTEM) images (Figure 9E,F). It is worthy to note that mesoporous carbon from MP-CS-36* shows bimodal-pores with detectable sizes of 2.6 and 5.8 nm calculated from N_2 sorption isotherms (Figure 10) in the case TEOS and is fully hydrolyzed and cross-

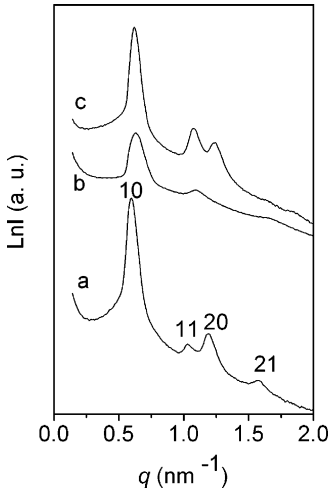

Figure 8. SAXS patterns of the mesoporous nanocomposite MP-CS-36*: (a) calcined at 900 °C in N_2, (b) mesoporous carbon MP-C-36*, and (c) mesoporous silica MP-S-36* derived from (a) after removal of silica and carbon, respectively.

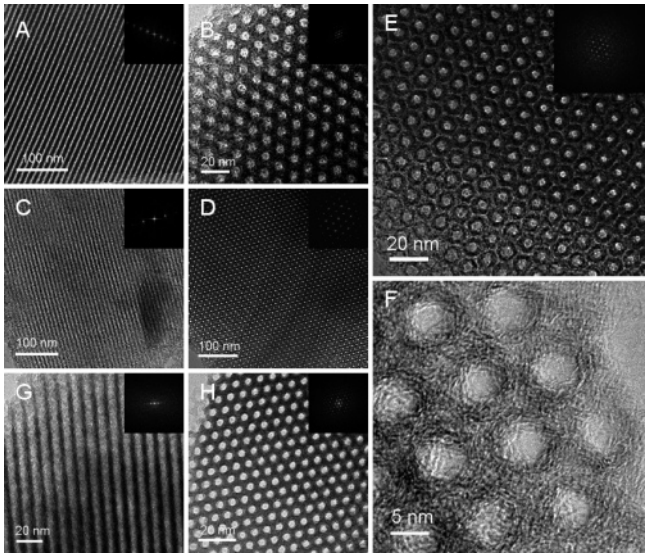

Figure 9. TEM images of mesoporous nanocomposite MP-CS-36* calcined at 900 °C in N_2 (A and B), mesoporous carbon MP-C-36* (C and D), and mesoporous silica MP-S-36* (G and H), and HRTEM images of carbon MP-C-36* (E and F), viewed from the [110] (A, C, G) and [001] (B, D, E, F, H) directions. The insets are the corresponding FFT diffractograms.

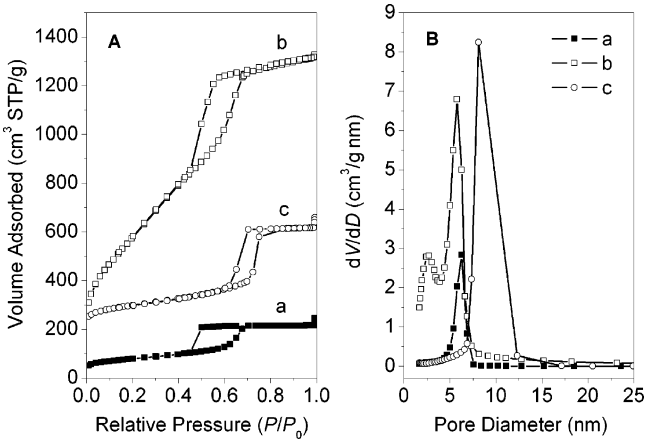

Figure 10. N_2 sorption isotherms (A) and pore size distribution curves (B) of the mesoporous nanocomposite MP-CS-36*: (a) calcined at 900 °C in N_2, (b) mesoporous carbon MP-C-36*, and (c) mesoporous silica MP-S-36*. The isotherms for silica are offset vertically by 200 cm^3/g.

linked by acid catalysis. It is similar to that for CMK-5, which is a tubular mesoporous carbon replica prepared by using mesoporous silica SBA-15 as a hard template.[26] TEM images give further evidence for bimodal pores. Many voids on the walls are observed (Figure 9D and E), which are similar to the character of CMK-5. It suggests the existence of interpenetrating pores with uniform distribution on carbon pore walls.

The primary pores of 5.8 nm in mesoporous carbon from MP-CS-36* are equal to that of the carbon from MP-CS-36 whose mother nanocomposites have the same mass C/SiO_2 ratios. Yet the complementary pores on the walls from dissolution of silica frameworks in the carbon from MP-CS-36* are bigger and more uniform than the latter. It can be assigned to the larger 3-D silica networks when the aging time of TEOS is prolonged in an acidic solution and the polymerization and cross-linking degrees are improved. Larger-domain silica aggregations can then be obtained, implying the "reinforcing-steel-bar" becomes wider. The bulky silica aggregation in carbon−silica nanocomposites would bring about larger mesopores (2.6 nm) on derived carbon pore walls after etching silica. The bimodal mesoporous carbon has a high BET surface area of 2130 m^2/g and a large pore volume of 2.02 cm^3/g. To the best of our knowledge, this is the first report of well-ordered open mesoporous carbon frameworks with bimodal pore structure by a surfactant-assembly approach.

4. Conclusion

A triconstituent co-assembly strategy to prepare highly ordered mesoporous polymer−silica and carbon−silica nanocomposites is first demonstrated, by using resols and pre-hydrolyzed TEOS as organic and inorganic precursors and triblock copolymer F127 as templates via the EISA approach. This approach is simple, low-costing, and easily reproducible. The resultant constituent distributions and the structural and textual properties of the final mesoporous products are controllable. An interpenetrating framework with "reinforced-concrete"-like structures for the nanocomposites has been proposed for the first time. Because of the presence of rigid silicates that act as a "reinforcing-steel-bar", the framework shrinkage is very small, and the pore sizes are as large as 8.5 nm for polymer−silica and 6.7 nm for carbon−silica nanocomposites. The actual control on the co-assembly of resols and silicates is indicated by the fact that the polymer/SiO_2 and C/SiO_2 mass ratios of the constituents can be ranged from zero to infinity. It is also reflected by the attainment of either pure silica frameworks or carbon frameworks. Combustion in air at 550 °C can remove carbons in the carbon−silica nanocomposites and result in mesoporous silicas with large meso-tunnels. Simultaneously, silica can be etched by HF solution, and ordered carbon frameworks can be obtained with large pores of ∼6.7 nm, pore volumes of ∼2.02 cm^3/g, and high surface areas of ∼2470 m^2/g. Besides the primary uniform large pores, plenty of complementary small pores exist in carbon pore walls, which contribute to much of the surface area. Complementary pores can be simply adjusted by tuning hydrolysis and condensation degrees of silicates before the co-assembly. Prolonging aging time of TEOS in the synthesis of nanocomposites can generate highly ordered mesoporous carbon frameworks with evident bimodal pores at 2.6 and 5.8 nm. This approach may be generally extended to a wide range of organic and inorganic nanocomposites, such as metal−polymer, conductive polymer−inorganic oxides.

Acknowledgment. This work was supported by the NSF of China (20233030, 20421303, 20407014, and 20521140450), State Key Basic Research Program of PRC (2001CB610506), Shanghai Sci. & Tech. Committee (05DZ22313, 03527001, 04JC14087, and 03QF14037), LG Co., Unilever Research China, and Shanghai HuaYi Chemical Group. Y.W. thanks the China Post-Doc Scientific Fund. We thank Dr. S. H. Xie and L. J. Zhang for experimental and characterization assistance.

Supporting Information Available: Complete ref 12. SAXS patterns, N_2 desorption isotherms, and pore size distribution curves of as-made, polymer−silica and carbon−silica nanocomposites MP-CS-46. *V*−*t* plots of nanocomposite MP-CS-46, mesoporous carbon, and silica. TG analyses of triblock copolymer F127, and as-made, polymer−silica and carbon−silica nanocomposites MP-CS-46 and MP-C-46. SAXS patterns of mesoporous pure silica (MP-CS-0). XRD patterns and Raman spectra of the mesoporous carbons derived from MP-CS-46 and MP-CS-36*, respectively. This material is available free of charge via the Internet at http://pubs.acs.org.

JA0633518